ADVANCED VEHICLE MOTION CONTROL OF ELECTRIC VEHICLE BASED ON THE FAST MOTOR TORQUE RESPONSE

Shin-ichiro Sakai, Univ. of Tokyo, Dept. of Elec. Eng., Japan
Yoichi Hori, Univ. of Tokyo, Dept. of Elec. Eng., Japan

Abstract

One remarkable merit of Electric Vehicles (EVs) is the electric motor's excellent performance in motion control. This merit can be summarized as: (1) torque generation is very quick and accurate, (2) output torque is easily comprehensible, (3) and motor can be small enough to be attached to each wheel. To utilize these advantages of EVs, we have carried out some studies on motion control of EVs. First of this paper, the feedback control of wheel velocity is discussed. The controller increases the wheel inertia equivalently and prevents the sudden rise of slip ratio. Experiments with actual EV and slippery road confirmed this effect. We assume that this method should be some minor loop controller. From such viewpoint, we discuss on two applications. One is concerning with lateral motion stability. Our simulation results show that unstable lateral motion on slippery curve can be stabilized with "4 wheel-motored" EV, if the wheel velocity controller is applied to each wheel as "autonomous" stabilizer. The other application is cooperative control of regenerative control and hydraulic ABS. Regenerative braking torque is controlled to have "large" inertia against hydraulic braking torque. This minor loop controller enhances the short-time dynamics of ABS and decreases the braking distance.

1. Introduction

Recently, electric vehicles (EVs) have attracted great interests as a powerful solution against environmental and energy problems. With improvement of motors and batteries, some pure EVs (PEVs) with only secondary batteries have already achieved enough performance. Hybrid EVs (HEVs), like Toyota Prius, are going up to the commercial products. Fuel cell EVs (FCEVs) will possibly be a major vehicle in the 21st century.

From the viewpoint of electric and control engineering, EVs have evident advantages over conventional internal combustion engine vehicles (ICVs). These advantages can be summarized as:

1. **Torque generation is very quick and accurate, for both accelerating and decelerating.**

   This should be the essential advantage. ABS (antilock brake system) and TCS (traction control system) should be integrated into "total TCS", since a motor can both accelerate or decelerate the wheel. Its performance should be advanced one, if we can fully utilize the fast torque response of motor.

2. **Output torque is easily comprehensible.**

   The second advantage will contribute a great deal to the road condition estimation. There exists little uncertainty in driving or braking torque inputted by motor, compared to that of combustion engine or hydraulic brake. Therefore, simple "driving force observer" can achieve a real-time observation of driving/braking force between the tire and road surface [1] [2].

3. **Motor can be attached to each wheel.**

   Distributed motor will possibly enhance the performance of DYC (direct yaw moment control) [3] [4]. The yaw moment can be generated more easily and precisely. Even the anti-directional torque generation is possible on left and right wheels.

On the other hand, the control engineering is now developed. If the actuator is fast enough as motor, we can fully apply these advanced theories. Metaphorically speaking, we can control EVs precisely as robots. However, only a few papers were published on this issue [5].

In this paper, we carried out some basic studies mainly on issue 1. To utilize the fast torque response, feedback control of wheel velocity is discussed. Generally speaking, such feedback controller can change the plant dynamics. Here authors attempt to increase the wheel inertia equivalently during the wheel skidding. Note that this is a minor loop controller, based on only the wheel velocity. Section 3 describes this method with experimental results. In section 4, effect of this method on vehicle lateral stability is studied. Another application of motor minor-loop control is introduced in section 5. This part discusses on the cooperative control of regenerative brake and hydraulic ABS. Section 6 concludes this paper.
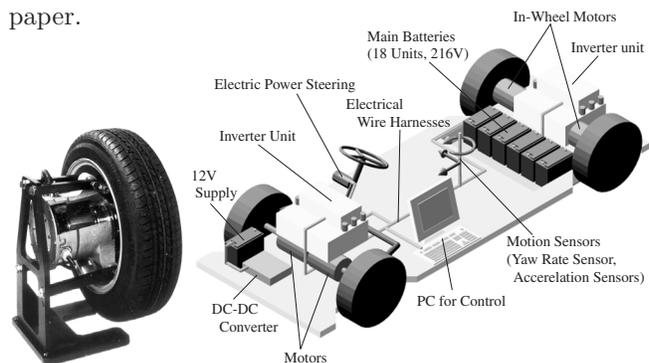

Figure 1. In-wheel motor and our new EV with four in-wheel motors.

2. Wheel velocity controller for skid prevention

In this section, the wheel velocity controller for skid prevention is discussed. The starting point of this idea is to utilize the knowledge on motion control, which is based on the motor control. In general, the feedback controller can change the dynamics of plant, or we can re-design the plant dynamics. For example, the plant can be insensitive against disturbance if appropriate feedback controller is applied. Such feedback control requires fast response of actuator, and so it should be suitable to utilize EV's advantage. So, how we should design the controller or plant dynamics for skid prevention? This is the main topics in this section.

2.1. Slip phenomena and linear slip model

Ordinary, slip ratio λ is used to evaluate the "slip". Slip ratio λ is defined as,

$$\lambda = \begin{cases} \dfrac{V_w - V}{V_w} & \text{: for accelerating wheel,} \\[2mm] \dfrac{V_w - V}{V} & \text{: for decelerating wheel,} \end{cases} \quad (1)$$

where V is the vehicle chassis velocity. V_w is the velocity equivalent value of wheel velocity, $V_w = r\omega$, where r, ω are the wheel radius and wheel rotating velocity, respectively.

With simple one wheel model (Fig. 2), the motion equations of wheel and chassis can be obtained as

$$M_w \frac{dV_w}{dt} = F_m - F_d(\lambda), \quad (2)$$

$$M \frac{dV}{dt} = F_d(\lambda), \quad (3)$$

if air resistance on chassis and rotating resistance on wheel are both negligible. M and M_w are the vehicle weight and the mass equivalent value of wheel inertia, respectively. F_m is the force equivalent value of accelerating/decelerating torque, generated by engine, hydraulic brake system or motor. F_d is the driving/braking force between the wheel and the road. This F_d has nonlinear dependence on the slip ratio λ, such as in Fig. 3 [1].
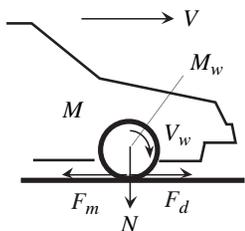

Figure 2. One wheel model.

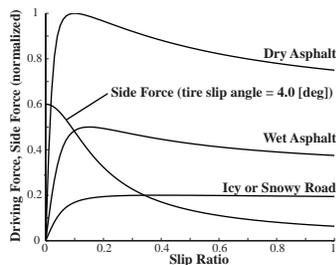**Figure 3.** $\mu - \lambda$ curve.

---

[1] $\mu = F_d/N$, where N is the normal force on the wheel.

For the controller design process, linear skid model from (1)-(3) and $F_d(\lambda)$ in Fig. 3 is derived. Nonlinearity exists in $F_d(\lambda)$ or $\mu - \lambda$ curve, therefore, perturbation equation for $F_d(\lambda)$,

$$\Delta F_d = N\Delta\mu = Na\Delta\lambda \quad (4)$$

$$= a\left(\frac{\partial\lambda}{\partial V}\Delta V + \frac{\partial\lambda}{\partial V_w}\Delta V_w\right) \quad (5)$$

$$= -\frac{1}{V_{w0}}\Delta V + \frac{V_0}{V_{w0}^2}\Delta V_w \quad (6)$$

is used here. The parameter a is the gradient of $\mu - \lambda$ curve,

$$a = \left.\frac{\partial\mu}{\partial\lambda}\right|_{(V_0, V_{w0})}. \quad (7)$$

V_{w0}, V_0 are the wheel velocity and chassis velocity at the operational point, respectively. With (1)-(3) and (6), the transfer function from motor torque F_m to the wheel velocity V_w is

$$P(s) = \frac{\Delta V_w}{\Delta F_m} = \frac{1}{(M_w + M(1-\lambda_0))s}\frac{\tau_w s + 1}{\tau_a s + 1}, \quad (8)$$

where

$$\tau_a = \frac{M_w V_{w0}}{aN}\frac{M}{M(1-\lambda_0) + M_w}, \quad \tau_w = \frac{MV_{w0}}{aN}. \quad (9)$$

λ_0 is a slip ratio at the same operational point (V_0, V_{w0}).

From (8)-(9), the most simple model for almost adhesive wheel ($\lambda_0 \ll 1.0$), $P_{\text{adh}}(s)$, can be described as

$$P_{\text{adh}}(s) = \frac{1}{M + M_w}\frac{1}{s}. \quad (10)$$

On the other hand, for the completely skidding wheel ($\lambda \simeq 1.0$), the dynamics seems to be $P_{skid}(s)$,

$$P_{\text{skid}}(s) = \frac{1}{M_w}\frac{1}{s}. \quad (11)$$

2.2. Controller design

One dominant phenomenon in the wheel skidding is the rapid change of wheel rotating velocity. During the acceleration, the wheel velocity rapidly increases with wheel skidding, and during the deceleration it rapidly drops due to the wheel lock. Eq. (10) and (11) describe that sudden drops of wheel equivalent inertia causes the rapid change of wheel velocity. Based on this viewpoint, we design the feedback controller of Fig. 4 [6]. The transfer function from acceleration command F_m^* to wheel velocity V_w with this controller is as follows:

(1) If wheel is adhesive, i.e., $P(s) = P_{\text{adh}}(s)$,

$$\frac{V_w}{F_m^*} = P_{\text{adh}}(s). \quad (12)$$

Therefore, the wheel dynamics against the acceleration/deceleration command is same as the original one. Feedback controller does nothing for adhesive wheel.

(2) If wheel is skidding, i.e., $P(s) = P_{\text{skid}}(s)$,

$$\frac{V_w}{F_m^*} = \frac{\tau s + 1}{\tau s + 1 + K_p \frac{M}{M+M_w}} \frac{1}{M_w s}. \tag{13}$$

For the low frequency region $\omega \ll 1/\tau$,

$$\frac{V_w}{F_m^*} = \frac{1}{\frac{(1+K_p)M+M_w}{M+M_w} M_w s} \tag{14}$$

Eq. (14) shows that the feedback controller modifies the wheel equivalent inertia for skidding wheel. For example, this transfer function comes to be

$$\frac{V_w}{F_m^*} = \frac{1}{(M+M_w)s} = P_{\text{adh}}(s), \tag{15}$$

if feedback gain K_p is chosen to be

$$K_p = \frac{M+M_w}{M_w}. \tag{16}$$

Fig. 5 shows the bode diagram of V_w/F_m^*. Upper graph plots V_w/F_m^* for wheel without controller, i.e., plots $P_{\text{adh}}(s)$ and $P_{\text{skid}}(s)$. If the controller of Fig. 4 is applied with K_p of (16) and $\tau = 0.1[s]$, these transfer functions change into the ones in lower graph. These figures clearly indicate that the dynamics of skidding wheel comes to be almost same as that of adhesive wheel, the "heavy" wheel. The wheel with proposed controller is insensitive for slip phenomena.
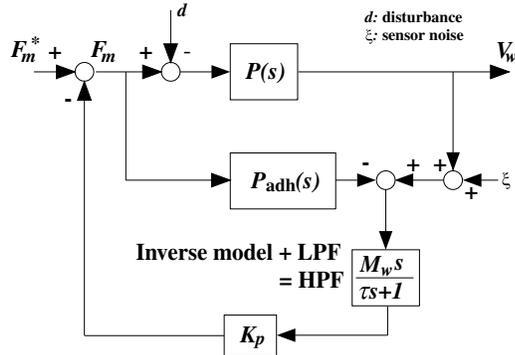

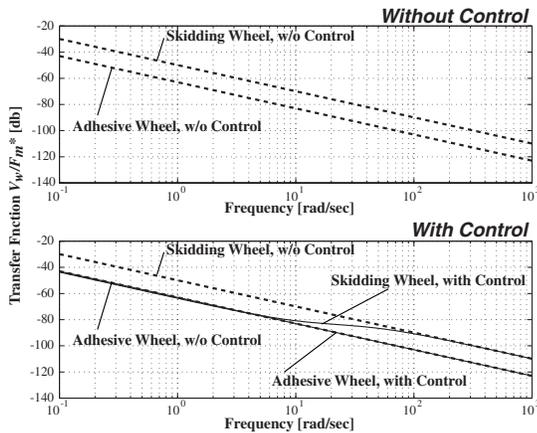**Figure 4.** Block Diagram of wheel velocity controller.

Figure 5. Bode diagram of V_w/F_m^*.

2.3. Experimental results

Experiments were carried out to confirm the proposed method. These experiments were carried out with "UOT Electric March-I", which is our laboratory-made EV (Fig. 6). The specification of this EV is shown in Tab. 1. To examine the effect of wheel velocity control for skid avoidance, slippery low μ road is required. We put the aluminum plates of 14[m] length on the asphalt, and spread water on these plates (Fig. 7). The peak μ of this test road is about 0.5. This value was estimated based on some other experimental results.

This "UOT Electric March-I" has one limitation on the experimental condition. This EV has a series-wound DC motor and an one-quadrant chopper. It means that the electric brake is impossible with our vehicle. Therefore, we carried out the skid prevention for accelerating vehicle, like skid prevention with TCS.

Table 1. Specifications of "UOT Electric March I".

Motor	DC Motor
Rated Power(5 min.)	32.5[kW] (44.3[HP])
Max. Torque	85[Nm]
Gear Ratio	13.5
Battery	**Lead Acid**
Nominal Capacity	92[Ah]
Weight	27.5[kg](for 1 unit)
Total Voltage	120[V] (with 10 units)
Chassis	**Nissan March**
Weight	1000[kg]
Wheel Inertia	21.1[kgm^2]*
Wheel Radius	0.26[m]
CPU	**i386, 20[MHz]**
Encoder(front/rear)	1800/120[ppr]

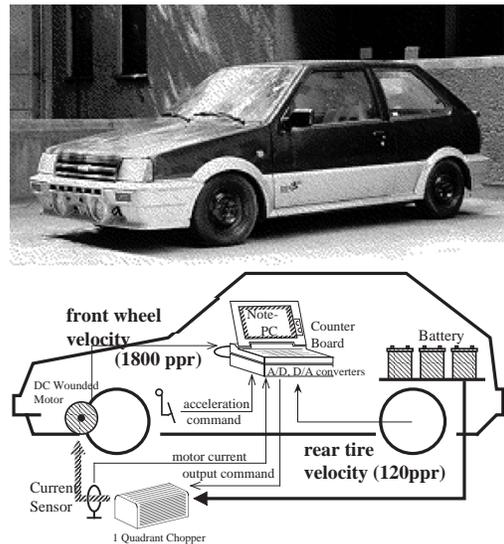* ... Including the rotor of motor, affected by gear ratio.

Figure 6. Our handmade EV, "UOT Electric March-I".

Fig. 8 shows the time responses of slip ratio. In these experiments, vehicle accelerated on the slippery test road, with lineally increasing motor torque. Without control, the slip ratio rapidly increases. On the contrary, the increase of slip ratio is relatively slow with proposed control. Fig. 9 plots the wheel and chassis speed. It shows the wheel velocity's insensitivity to the slip status. In other words, the wheel equivalent inertia during the wheel skidding comes to be "heavy" with wheel velocity control, thus the rapid increase of slip ratio can be suppressed. The simulation results almost agree with the experimental results. The difference were caused by:

1 The motor current was saturated in the experiments, with high V_w such as $\lambda = 0.6$.

2 At about 5.5[s], the EV reached at the end of the slippery test road and ran again on the dry asphalt.

This agreement indicates the reliability of simulations in the following sections.
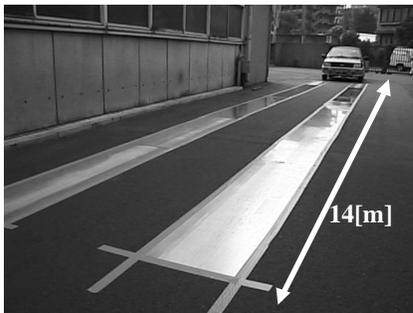

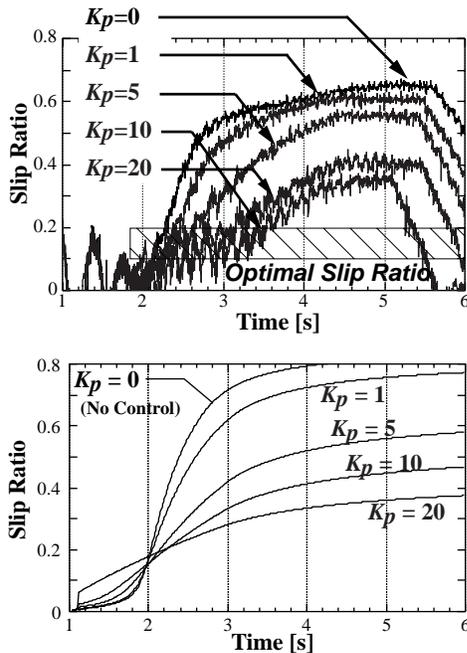**Figure 7.** Test low-μ road for experiments.

Figure 8. Effect of wheel velocity control for skid prevention with $\tau = 0.1$[s]. (Upper Fig.: Experimental results / Lower Fig.: Simulation results)

As mentioned above, the feedback controller changes the wheel dynamics as shown in Fig. 5, then the serious skid is prevented. Therefore, this effect depends on $P_{\rm adh}/P_{\rm skid}$. It can be evaluated about 5.0, which is calculated with M and M_w for our EV "UOT Electric March-I". Experimental results of Fig. 10 shows that, the growth rate of slip ratio decreased about five times. It means that this controller makes the "slip" about five times as slow as the original dynamics. This experimental result confirms that our controller design process was appropriate one.

Note that this method cannot be the complete skid prevention controller by itself. Proposed controller suppresses the rapid growth of slip ratio, however, the slip ratio can exceed the stable limit (Fig. 8). Therefore, we suggest this method as a minor-loop controller, to improve other method like conventional ABS or skid detection technique with EV [7].
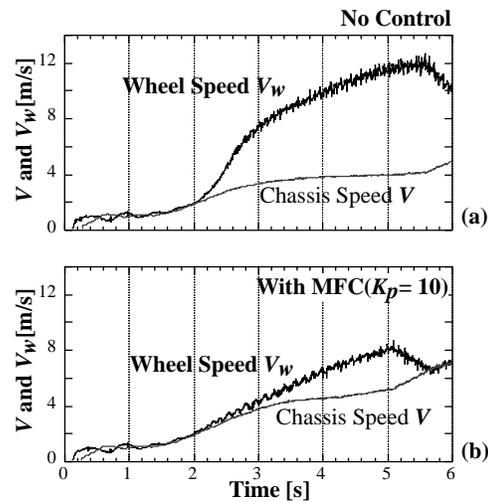

Figure 9. Wheel and chassis velocity. With control (upper fig.) and without control (lower fig.).
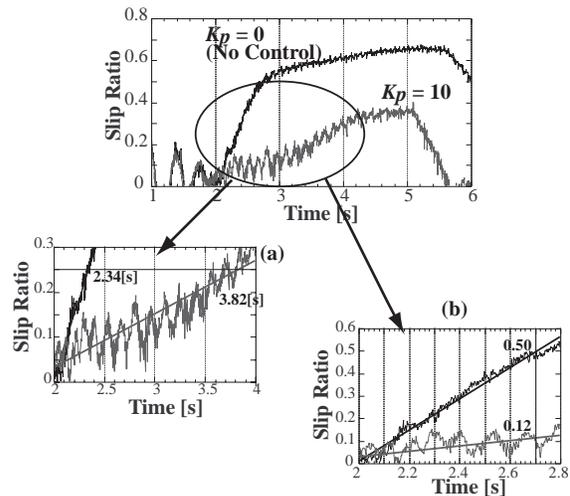

Figure 10. Effect of "slow" slip growth with proposed method.

3. Lateral motion stabilization with wheel velocity controller

In the previous section, wheel velocity feedback was discussed. With this method, wheel seems to have heavy inertia equivalently during slip. This suppresses the rapid increase of slip ratio. Then, what will happen if we apply such method for vehicle in cornering?

As commonly known, the vehicle lateral motion can be sometimes unstable. This instability occurs in such situation as rapid braking during turning the curve, especially with slippery road condition with snowy or rainy weather. Here we assume that the target EV is equipped one motor per one wheel. In-wheel motor is a typical example(Fig. 1). With such motor, the wheel velocity can be controlled in each wheel independently. Our simulation results (Fig. 11-13) show that this "4 wheel-MFC" can enhance the vehicle's lateral stability. Chassis's 3-DOF nonlinear motion, four wheel's rotation and dynamic load distribution are calculated in these simulations. Parameters in these simulations are shown in Tab. 2.
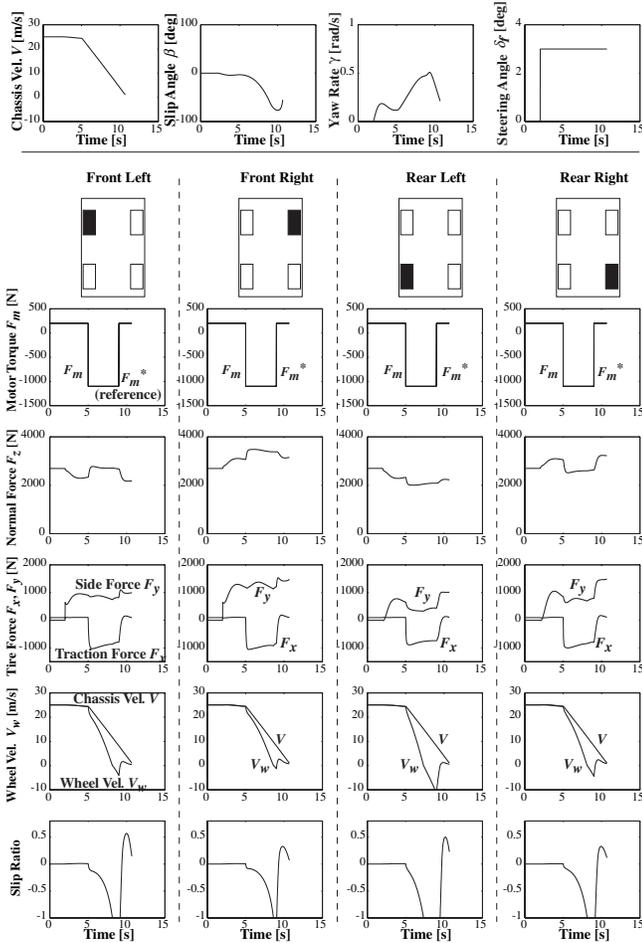
In these simulations, the vehicle starts running on the slippery road ($\mu_{\text{peak}} = 0.5$), turning left with steering angle $\delta_f = 3$ [deg]. Then at 5.0 [sec], the driver inputs rapid braking torque $F_m = -1100[\text{N}]$ on each wheel. This torque exceeds the tire performance. Therefore, the wheel skid occurs and the chassis starts the spin motion, although the driver stops braking at 9.0 [s]. This wheel skidding is serious at rear-left wheel especially, since the center-of-gravity is shifted and the load distribution varied. On the contrary, if the wheel velocity controller is applied independently for each wheel, such dangerous spin motion is prevented. The rear-left wheel's torque is most reduced automatically, and this indicates the autonomy stability effect of this method. Note that this method uses only wheel velocities as feedback signals, therefore, differs considerably from conventional methods like DYC [3] [8]. The autonomy stabilization of each wheel, which is achieved with wheel velocity control, enhances the stability of vehicle lateral motion on slippery road. Experimental studies should be carried out for further studies. We are now manufacturing actual EV with four in-wheel motors for this purpose (Fig. 1).
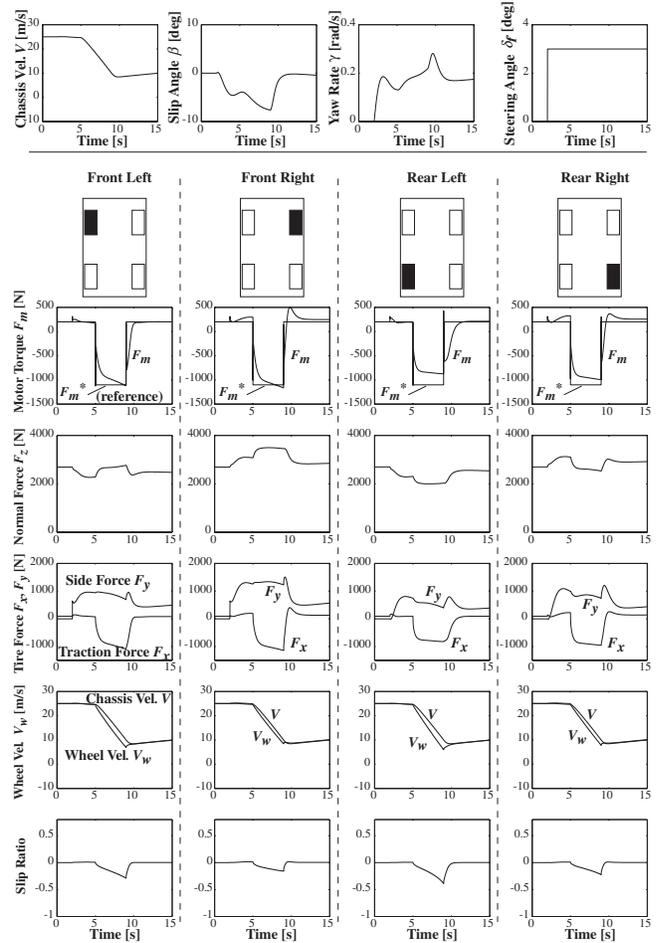

Figure 11. Example of unstable vehicle lateral motion. This is the simulation results of rapid braking on slippery road, during turning the curve. No feedback controller is applied ($K_p = 0$).

Figure 12. Simulation for the same situation as Fig. 11. Wheel velocity controller ($K_p = 5.0$) is applied for each wheel. Rapid lock of each wheel is suppressed, especially in rear-left wheel. This maintains the vehicle stability.

Figure 13. Stabilization effect of "controlled four wheels" is visualized with vehicle's trajectory. The upper one is the results of Fig. 11, and the bottom one is of Fig. 12.

Table 2. Parameters in the lateral motion simulation.

M	chassis weight	1100 [kg]
I	chassis moment	3760 [kgm^2]
F_{a0}	coefficient for air resistance	0.55 [Ns^2/m^2]
d_f	tread (front)	1.36 [m]
d_r	tread (rear)	1.33 [m]
l_f	COG - front axle length	1 [m]
l_r	COG - rear axle length	1.36 [m]
SM	static margin	0.076
M_w	wheel inertia (mass equivalent)	37.0 [kg]
r	wheel radius	0.26 [m]
F_{r0}	coefficient for rolling resistance	107.8 [Ns/m]
K_p	feedback gain of controller	0 / 1.0 / 5.0
τ	time constant of controller	0.1 [s]
longitudinal load distribution (at 1G)		3:7
lateral load distribution (at 1G)		3:7
Tire Model:	Magic Formula with λ Method.	

4. Regenerative braking control cooperating with hydraulic ABS

With motor or regenerative braking, fast feedback control can be applied as mentioned above. Such controller can change the dynamics of wheel, for example, change the wheel's equivalent inertia to be quite heavy.

In this section, regenerative braking control cooperating with hydraulic ABS is introduced. In most EVs or HEVs, regenerative braking is generally used with hydraulic braking system. Pure electric braking is not applied at this moment. The reason is the maximum torque limitation of motor, batteries' SOC (state of charge), or expectation for the reliability of mechanical systems. Thus if someone attempt to apply the anti skid method with motor control, cooperation or interference between regenerative and hydraulic braking must be considered. ABS was well studied and practically applied [9]. Most conventional systems sense the acceleration of wheel velocity and/or slip ratio, and control the wheel brake cylinder's hydraulic pressure. However, it is still difficult to prevent large drop of wheel velocity at the beginning of control [10]. Therefore, we intend to improve such short-time performance of ABS with regenerative brake control, i.e., motor control. Here we show some basic idea to achieve such control.
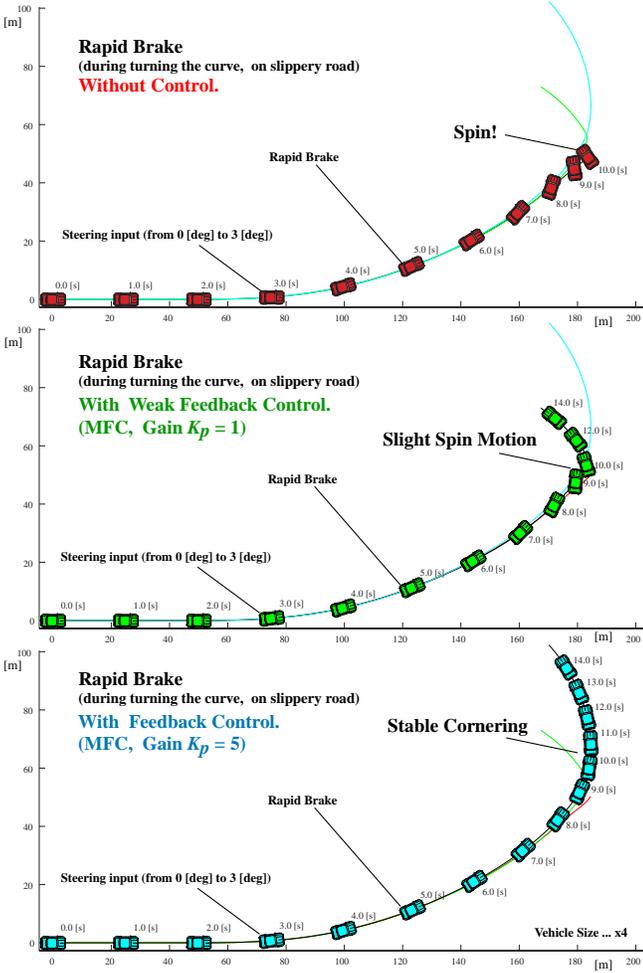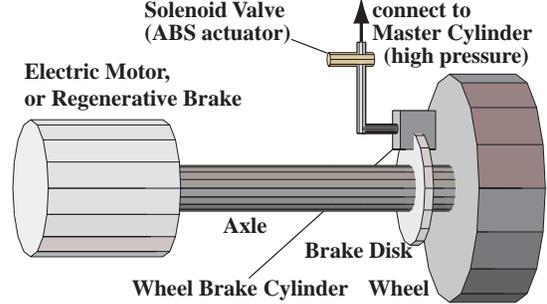

Figure 14. Hydraulic and regenerative brake.

4.1. Regenerative braking controller design

One of the problems of hydraulic ABS is the delay in the skid detection or actuator response. Thus, here we aim to compensate the wheel's short-time dynamics within such delay time.

Fig. 15 shows the block diagram of proposed controller. Hydraulic system generates braking torque F_{ABS}, based on the hydraulic braking torque reference F_{ABS}^*. The total braking torque F_{brake} is

$$F_{\text{brake}} = F_{\text{motor}} + F_{\text{ABS}}, \qquad (17)$$

where F_{motor} is the regenerative braking torque, output of proposed controller. We assume the purpose as below:

(1) If wheel is adhesive: ABS controller do nothing, therefore, $F_{\mathrm{ABS}} = F_{\mathrm{ABS}}^* + \Delta$, where Δ denotes the uncertainty factor such as pad secular variation. **In this case, motor torque should be $F_{\mathrm{motor}} = F_{\mathrm{motor}}^*$.** Both F_{ABS}^* and F_{motor}^* are required by upper layer controller, which decides how to achieve the driver-requiring deceleration rate, with maximizing the energy efficiency of regenerative brake.

(2) If wheel is skidding: ABS controller works. **The actual F_{ABS} is assumed to be unmeasurable.** Energy efficiency of regenerative brake is not important issue in this case, therefore, no need to achieve $F_{\mathrm{motor}} = F_{\mathrm{motor}}^*$. The feedback controller should varies F_{motor} actively and dynamically, to improve the ABS performance. **Constraint: the feedback controller have no information about ABS controller, and we can do nothing on ABS control algorithm.**

In addition, **regenerative brake controller is assumed to be a single controller.** The algorithm is always the same, and it is not switched depending on the ABS on/off status. For these purposes and constraints, we take a controller design strategy which is quite similar to the previous one in Sec. 2. This feedback controller can be described with $P_n(s)$ and $Q(s)$,

$$P_n(s) = \frac{1}{(M + M_w)s}, \quad Q(s) = Ms\frac{1}{\tau s + 1}. \quad (18)$$

With these feedback controller and $\tau = 0.1$[s], the transfer function $H(s)$ from F_{ABS} to F_{brake} can be changed as Fig. 16. [2] Fig. 17 plots $H(s)P(s)$, which is the transfer function from F_{ABS} to V_w. These bode diagrams are calculated with simple wheel model $P_{\mathrm{adh}}(s)$ and $P_{\mathrm{skid}}(s)$, defined in (10) and (11), respectively.

The remaining problem of this controller is the steady-state gain for adhesive wheel, $H(0)_{\mathrm{adh}}$,

$$H(0)_{\mathrm{adh}} = \frac{M + M_w}{2M + M_w} \neq 1.0. \quad (19)$$

Eq. (19) means that the transmission of hydraulic braking torque is blocked with motor torque. To prevent this blocking, the feedforward controller C_{FF} is designed as,

$$
\begin{aligned}
C_{\mathrm{FF}}(s) &= \left(1 - H_{\mathrm{adh}}(0)\right)F_{\mathrm{ABS}}^* + F_{\mathrm{motor}}^* \\
&= \frac{M}{2M + M_w}F_{\mathrm{ABS}}^* + F_{\mathrm{motor}}^*. \quad (20)
\end{aligned}
$$

With this feedforward controller, the total braking torque F_{brake} during adhesive decelerating come to be

$$F_{\mathrm{brake}} = F_{\mathrm{motor}}^* + F_{\mathrm{ABS}}. \quad (21)$$

Note that response to both reference and disturbance ($= F_{\mathrm{ABS}}$) is concerned here, although response to only the reference was concerned in Sec. 2.
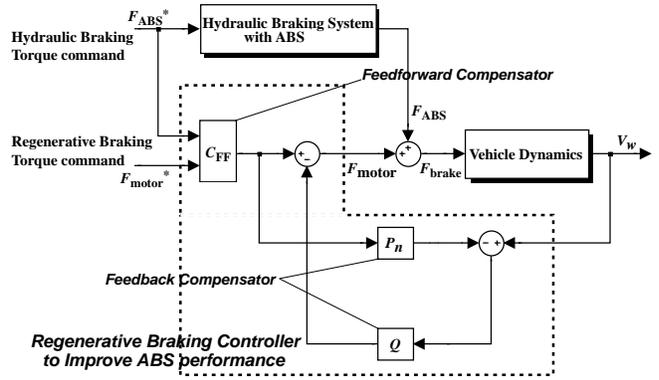
---

[2] Of course, $H(s)$ is a sensitivity function.
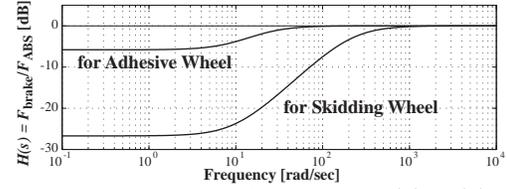

Figure 15. Block diagram of proposed controller.
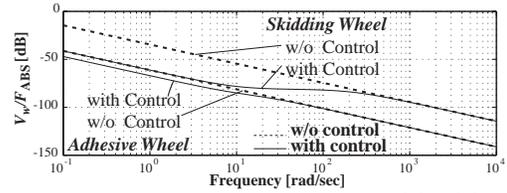

Figure 16. Bode diagram of $H(s), G(s)$.

Figure 17. Bode diagram of $H(s)P(s)$.

Table 3. Parameters in the simulations.

Vehicle weight (M)	1100[kg]
Wheel inertia (M_w)	53.3[kg]
Dead time in skid detection (τ_{Ds})	50[ms]
Dead time in ABS torque response (τ_D)	20[ms]
1st order delay in ABS torque response (τ_m)	50[ms]
Max. of Hydraulic Braking torque	4000[N]
Max. of Regenerative Braking torque	2000[N]
1st order Delay in Motor torque response	1[ms]
Vehicle model :	One wheel model
Tire model :	Magic Formula

4.2. Simulation results

Simulations are carried out to confirm the effectiveness of proposed controller. Tab. 3 shows the parameters. ABS controller is modeled simply as bang-bang controller, with time delay in Tab. 3 [11].

Fig. 18 shows the simulation results with adhesive road condition ($\mu_{\mathrm{peak}} = 1.0$). The motor generates the commanded regenerative braking torque, which is required by upper layer controller, for example to maximize the energy efficiency. The feedback controller does not block or interfere with the hydraulic braking torque.

Fig. 19 shows the results with slippery road condition ($\mu_{\mathrm{peak}} = 0.5$). The left column shows the results with only hydraulic ABS, and the right column shows

the results with hydraulic ABS and proposed controller. Bottom figures are the comparison of these methods. These figures show that the slip ratio oscillation can be suppressed with proposed regenerative brake controller. The braking force is enlarged by this effect, therefore, the braking distance can be reduced by 20 %. However, the ABS controller in this simulation is quite simple and not practical one. The results in this paper just shows the basic idea, and further studies should be carried out.
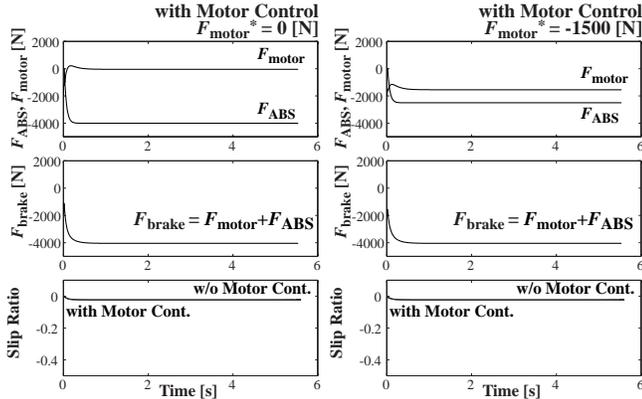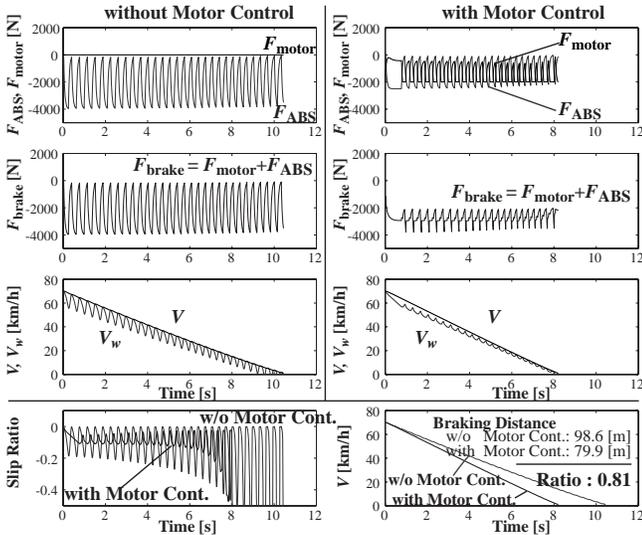

Figure 18. Simulation results with adhesive road.

Figure 19. Simulation results with slippery road. $F_{motor}^* = $ -1500 [N]
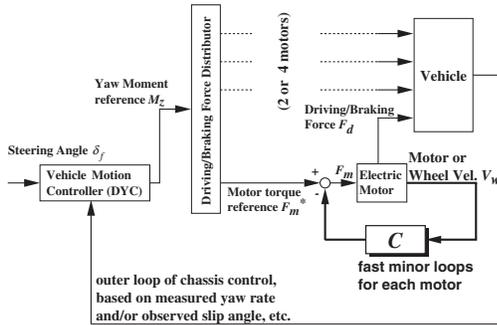

Figure 20. Our concept: minor-loop motor controller.

5. Conclusion

In this paper, we described the advantage of EVs in motion control issue. The goal is to enhance the vehicle stability with feedback control of motors. We proposed the wheel velocity controller for skid prevention, and confirmed with experiments using actual EV. This controller can change the wheel's dynamics, or increase the equivalent inertia of wheel. Such feedback control is difficult with slow actuator like engine or hydraulic brake. The proposed feedback controller can enhance the vehicle lateral stability, as we showed with simulations. The motor control loop is a fast minor feedback loop in a total chassis control system, as depicted in Fig. 20. This minor loop will enhance the stability of upper layer chassis control system, such as DYC. Note that DYC can be easily applied in EV with two or four motors. We have almost manufactured such EV for experimental studies (Fig. 1). Another example of our concept, fast minor-loop with motor, was also shown. The novel regenerative braking controller was designed, and was confirmed to improve the performance of hydraulic ABS. The proper cooperation between slow ABS actuator and fast motor seems to be the interesting issue for further studies.

References

[1] Hideo Sado, Shin-ichiro Sakai and Yoichi Hori (1999), "Road condition estimation for traction control in electric vehicle", In *IEEE International Symposium on Industrial Electronics*, pp. 973–978, Bled, Slovenia.

[2] Shin-ichiro Sakai, Hideo Sado and Yoichi. Hori (2000), "Novel skid avoidance method without vehicle chassis speed for electric vehicle", In *Proc. International Power Electronics Conference*, Vol. 4, pp. 1979–1984, Tokyo.

[3] Yasuji Shibahata, et al. (1992), "The improvement of vehicle maneuverability by direct yaw moment control" In *Proc. AVEC '92*, No. 923081.

[4] Sumio Motoyama, et al. (1992), "Effect of traction force distribution control on vehicle dynamics" In *Proc. AVEC '92*, No. 923080.

[5] P.Khatun, C.M.Bingham, P.H.Mellor, and N.Schofield (1999), "Discrete-time ABS/TC test facility for electric vehicles" In *Proc. EVS. 16*, p. 75, Beijing.

[6] Y. Hori, Y. Toyoda, and Y. Tsuruoka (1998), "Traction control of electric vehicle: Basic experimental results using the test EV "UOT electric march" ", *IEEE Trans. Ind. Applicat.*, Vol. 34, No. 5, pp. 1131–1138.

[7] Shin-ichiro Sakai, Hideo Sado, and Yoichi Hori (1999), "Motion control in an electric vehicle with 4 independently driven in-wheel motors", *IEEE Trans. on Mechatronics*, Vol. 4, No. 1, pp. 9–16.

[8] Y. Furukawa and M. Abe (1998), "Direct yaw moment control with estimating side-slip angle by using on-board-tire-model", In *AVEC'98*, pp. 431–436.

[9] Taketoshi Kawabe, Masao Nakazawa, Ikuro Notsu, and Yoshito Watanabe (1996), "A sliding mode controller for wheel slip ratio control system" In *Proc. AVEC'96*, pp. 797–804.

[10] Yuzo Imoto, et al. (1998), "High-efficiency brake pressure controls in ABS" In *AVEC '98*, pp. 655–660.

[11] T. Tabe, N. Ohka, H. Kuraoka, and M. Ohba (1985), "Automotive antiskid system using modern control theory", In *Proc. IEEE IECON'85*, pp. 390–395, San Francisco, USA.